THE NEW INJECTOR DESIGN FOR THE UPGRADED RADLAC-II LINEAR ACCELERATOR*

M. G. Mazarakis, J. W. Poukey, S. L. Shope, D. E. Hasti
C. A. Frost, G. T. Leifeste, and D. L. Smith
Sandia National Laboratories, Albuquerque, NM 87185

ABSTRACT

The cathode field shaper, shank assembly, and magnetic field profile have been redesigned for the upgraded RADLAC-II configuration. The new design incorporates our most recent experimental observations, JASON code analysis, and simulation results with the newest version of particle-in-cell (PIC) code MAGIC. A conical field shaper was selected that starts at the cathode end plate with a 10-cm diameter cylinder and tapers smoothly to the cathode tip. The field shaper is 1-m long. Three interchangeable cone tips provide for different diameter cathode tips (1.2 cm, 1.9 cm, and 2.5 cm). The simulations show that a 40 to 50-kA annular cold beam can be produced with an rms transverse velocity component $\beta_\perp = 0.06$ and a radius r = 0.85 cm. The total cathode shank losses are drastically reduced and the previously observed beam halo completely eliminated. Experimental results are in good agreement with the design goals.

INTRODUCTION

The new injector is part of the extensive improvements incorporated in the upgraded version of the RADLAC-II linear induction accelerator.[1] These improvements aim at increasing the total energy and current output and producing a higher quality electron beam. The pulsed-power network was also redesigned, and the available energy was doubled by the addition of two more Marx generators. Now, the maximum voltage applied across the injector is 5 MV and the pulse FWHM is 50 ns. In addition, new magnetic field coils were installed, providing higher magnetic field strength (20-25 kG) and better field uniformity throughout the accelerator. A detailed description of the upgraded RADLAC-II accelerator is given in Ref. 2.

THE RADLAC-II INJECTOR

Old Design

Two electrically graded vacuum insulator stacks are connected in series to form the RADLAC-II injector cavity where the anode and cathode field shapers and the foilless diode electron source are located (Fig. 1). Each diode stack is powered by the same pulsed-power network as the post-accelerating cavities. The injector voltage is approximately equal to the sum of the voltages along the two diode stacks measured by the two resistive monitors (Fig. 1). The beam current is monitored by a Rogowski coil located 1.4-m downstream from the A-K gap of the foilless diode. The total current emitted by the cathode shank and by the cathode field shaper (Fig. 1) is measured by a larger Rogowski monitor surrounding the base of the field shaper inside the injector cavity.

The foilless diode is immersed in the axial magnetic field that guides the beam through the 10-m long vacuum line of the accelerator. The guiding field is produced by solenoidal coils surrounding the beam pipe. The original cathode field shaper design was for 6-MV, ~100-kA beams; therefore, different factors and parameters were of importance. Because of the large currents, reducing the inductance was the primary consideration. Accordingly, the anode and cathode field shapers were chosen to be cylindrical with 20-cm outer diameter, and the distance between them was kept as short as possible, requiring only a 15-cm long, 2.5-in diameter cathode shank. However, the beam currents could not provide magnetic insulation for the 20-cm field shaper in the fringing magnetic guide field, B_z, of the accelerator.

In addition to a large current flowing radially from the cathode field shaper, a significant current was emitted from the front surface, causing a deleterious effect on the beam quality. A fraction of this current entered the beam pipe causing beam halo and beam annulus filling-in.

Figure 2 is a JASON[3] code plot for the old field shaper. Only one diode stack is shown. The voltage across the second one is taken into account by properly adjusting the anode plate boundary conditions. This approach was used in order not to exceed the code memory capacity. More than half of the cylindrical surface of the cathode field shaper is electrically stressed above 200 kV/cm and capable of emitting electrons. This injector configuration, in particular the section of the stainless steel cylinder connecting the two insulating stacks, is reminiscent of a coaxial transmission line; thus, the formalism of Creedon model for self-magnetic insulation can be applied.[4,5] The minimum current required for load-limited magnetic cutoff is given by the expressions:

$$I_\ell = g\gamma_\ell^3 \,\ell n\left[\gamma_\ell + (\gamma_\ell^2 - 1)^{1/2}\right] ,$$
$$\gamma_0 = \gamma_\ell + (\gamma_\ell^2 - 1)^{3/2}\,\ell n\left[\gamma_\ell + (\gamma_\ell^2 - 1)^{1/2}\right] , \qquad (1)$$

where $g = \left[\ell n \dfrac{R_2}{R_1}\right]^{-1}$ is a geometric factor.

The relativistic factor γ_ℓ is for electrons at the boundary of the electron sheath in the minimum current case. In the case of the old design, we have R_2 = 25 cm, R_1 = 10 cm and $\gamma_0 = 3\ \mathrm{MV}/mc^2 + 1$. The voltage of the outer metallic cylinder is half the total anode voltage and equal to 3 MV. These parameters give a I_ℓ = 78 kA, well below the 100 kA imposed by the foilless diode load. In addition, the critical current $I_c = 8400\ g\beta_0\gamma_0$, which assures that no electron will hit the outer cylinder, is 65 kA. The electron sheath corresponding to the I_ℓ = 78 kA extends outside the field shaper cylinder and up to equipotential surface of 443 kV (γ_ℓ = 1.887). If the A-K gap of the foilless diode is adjusted to produce 100 kA, the current sheath is further compressed down to 115-kV equipotential cylinder (γ_ℓ = 1.225). Hence, 100 kA was a large enough current to secure self-magnetic insulation for the old cylindrical surface. However, the fields at the edge of the cylinder still were very strong (up to 600 kV/cm) and caused the electrons of the sheath to escape the cylindrical surface then being accelerated to the anode plate. Although in the present experiments the voltage along the injector is only 5 MV, the minimum diode current required for magnetic insulation is I_ℓ = 67 kA and the critical current is 50 kA. Both are higher than the 40 kA required. To make things even worse, the fringing field of the guiding magnetic field weakens

*This work was supported by the U.S. DOE under contract DE-AC04-76DP00789 and by DARPA/AFWL under Project order AFWL86-154.

the self-magnetic insulation at the location where it is most needed, that is, near the end of the highly stressed cathode field shaper.

The above analysis has been verified by the PIC code MAGIC.[6] Figure 3 is a MAGIC simulation of the old cylindrical injector showing the amount and the location of the shank electron losses. With a total shank current of 145 kA only 35 kA appear as beam current. The larger current, 100 kA, escapes radially and strikes the stainless steel cylinder that connects the two insulating stacks. A smaller current, 10 kA, strikes the anode plate at the entrance to the beam pipe. This component disrupts the beam causing beam halo and annulus thickening to occur. Figure 4 shows the measured injector voltage and cathode shank current from the old injector geometry.

According to expression (1), a 40 kA current should provide a very good self-magnetic insulation for a cathode field shaper and shank of the same diameter equal to 2 cm. Indeed, the estimated minimum current, I_ℓ, is 24 kA and the critical current, I_c, is 20 kA. Figure 5 proves that this thin field shaper does in fact cut down the shank losses to 11 kA. The electrons leak from a very narrow shank region and move radially outwards to the cavity walls closely following the fringe lines of the B_z field.

Although this narrow shank appears satisfactory from the point of view of shank losses and beam quality,[7] it has some disadvantages: first, it is not rigid enough and therefore very difficult to keep aligned; second, it has considerable inductance and causes a large Ldi/dt reduction of the applied voltage at the A-K gap.

The New Injector Design

The new injector design adopted includes an excellent mechanical support which provides good flexibility in alignment, superior rigidity, and shot-to-shot stability for the cathode tip. The shank losses are as low as the ones experienced with the small radius straight cylinder, but the inductance is reduced. A conical design was chosen which starts at the cathode end plate with a 10-cm diameter cylinder and tapers off smoothly at the cathode tip. The total length of the cathode field shaper and shank is one meter. Three interchangeable cone tips provide for different diameter cathode shanks (1.2 cm, 1.9 cm, and 2.5 cm). The mechanical design has numerous openings at the outer surface for ample vacuum pumping. The half angle of the cone is 4° and the radius of the conical surface as a function of the distance from cathode end plate is such that it can provide magnetic insulation against radial emission all along its length. The magnetic field at the A-K gap is 20 kG.

Some radial losses occur again in a region of narrow axial extent where the fringe field lines of the applied solenoidal field, B_z, intercept at an almost right angle with the shank surface. The region is where the magnetic insulation would be expected to fail if there were not a self-magnetic field B_θ. On the anode side of the region, magnetic insulation is obtained due to the guiding magnetic field B_z. Figure 6 shows the equipotential surfaces for the conical injector as obtained by the JASON code, and Fig. 7 gives the electron map for the new injector geometry. A new version of MAGIC which includes subroutines allowing space-charge limited emission from slanted conducting surfaces was utilized for these simulations. The shank current losses are 20%.

The experimental results indicate good agreement between numerical simulation and measurements. Actually, the injector performs even better than predicted. The measured cathode shank current losses are only 5-11% instead of the 20%-30% expected from the MAGIC simulations. Beam currents range from 35 kA at 3.6 MV to 41 kA at 4.1 MV (Fig. 8). The cathode shank current for those shots were 37 kA and 45 kA. As shown by the time-integrated x-ray pinhole photograph (Fig. 9), the beam halo is eliminated and the beam is annular without any appreciable filling-in. Using the expression of Ref. 7:

$$\beta_\perp = \frac{(w-\alpha)B[kG]}{3.4\,\gamma}$$

where w is the beam annulus thickness and α the cathode tip annulus thickness, we estimate from Fig. 9 a $\beta_\perp \approx 0.10$.

CONCLUSIONS

A new injector for the upgraded RADLAC-II accelerator was designed and recently installed in the device. Creedon's model formalism and the JASON code proved quite useful in reducing the design options to a few. The final selection was based on numerical simulations. The adopted design was extensively analyzed and validated with the newest version of the particle-in-cell (PIC) code, MAGIC, that includes the slant geometry package.

The new RADLAC-II injector performs according to the design goals. The previously observed excessive electron losses have been eliminated. The total measured shank current is only 5-10% higher than the 40-kA beam current. A high quality annular beam is generated with a $\beta_\perp$ of 0.1 and normalized emittance equal to 0.8 rad-cm. The mechanical support provides excellent rigidity, good alignment means, and shot-to-shot stability. The cathode tip can be centered to within 0.1 mm and remains in alignment after more than 50 shots. Thus, the major problems from the old injector concerning cathode alignment, mechanical stability, current efficiency, and beam quality have been adequately solved.

REFERENCES

1. M. G. Mazarakis et al., "RADLAC-II Accelerator Beam Experiments," Proc. of the IEEE Particle Accelerator Conf., (Washington, DC, March 16-19, 1987), CH2387-9/87/0000-0908.
2. S. L. Shope et al., "The Upgraded RADLAC-II Accelerator," this conference.
3. S. J. Sackett, "JASON-A Code for Solving General Electrostatics Problems User's Manual," LLL report UCID-17814. Revised by M. L. Kiefer, Sandia National Laboratories, Albuquerque, NM (1984).
4. J. M. Creedon, J. Appl. Phys. 48(3), 1070 (1977).
5. J. M. Creedon, J. Appl. Phys. 46, 2946 (1975).
6. B. Goplen, et al, "Users Manual for MAGIC/version-Sept. 1983, MRC/WDC-R/068," Mission Research Corp., Washington, D.C., (1983).
7. D. E. Hasti, et al., "RADLAC-II Upgrade Injector Experiments," SNLA SAND88-1032, Albuq., NM, 1988.

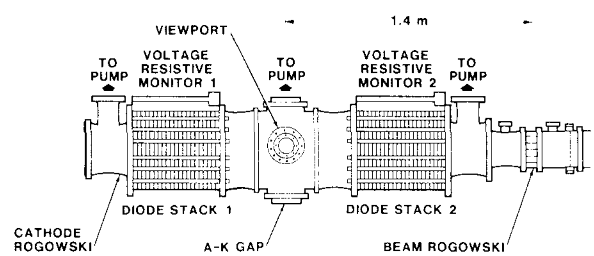

Fig. 1. RADLAC-II injector cavity.

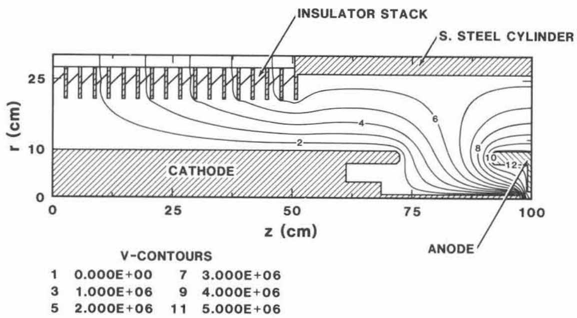

Fig. 2. Equipotential plot for the old cathode field shaper. The anode voltage is 5 MV.

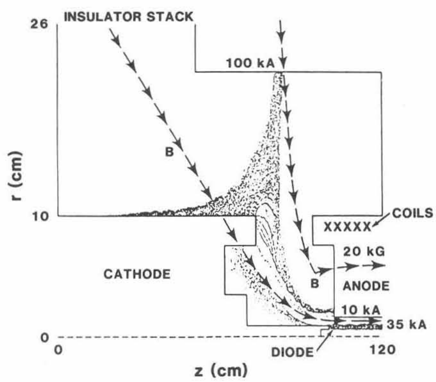

Fig. 3. Particle code simulation for the old injector geometry. The cathode shank current losses are 110 kA. The beam current is only 35 kA. The voltage is 5 MV. The arrows indicate two magnetic field flux lines.

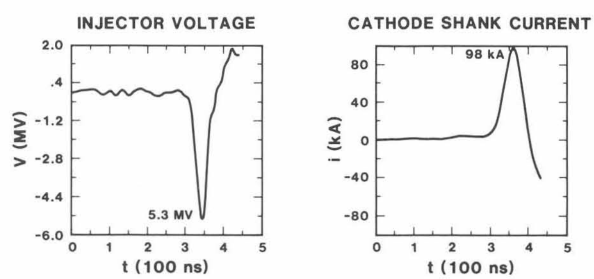

Fig. 4. Measured injector voltage and cathode shank current with the old injector.

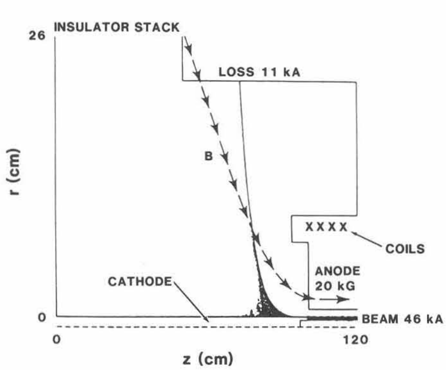

Fig. 5. Particle code simulation of the injector with a thin 2-cm in diameter cylindrical cathode field shaper and shank. The voltage applied to the A-K gap of the diode is 4 MV. The total cathode shank current is 57 kA. The beam current is 46 kA.

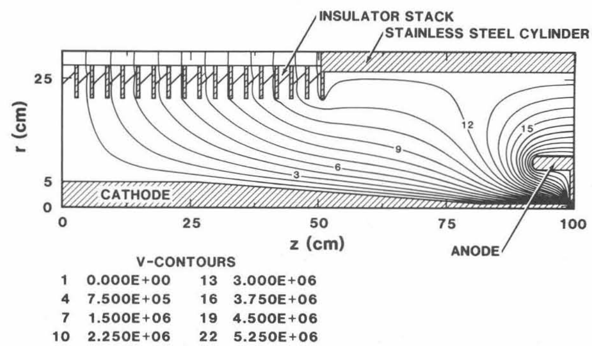

Fig. 6. Equipotential plot for the new conical field shaper.

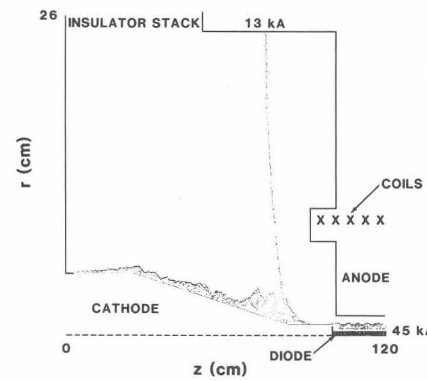

Fig. 7. Electron map for the new injector. The applied voltage to the A-K gap is 4.75 MV. All the electron losses occur radially and account only for 13 kA of the 58 kA total shank current.

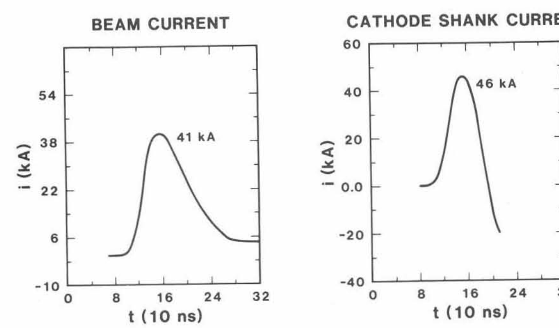

Fig. 8. Total shank and beam current for a 4.1 MV injector voltage. The shank current losses (=shank current minus beam current) are less than 11%.

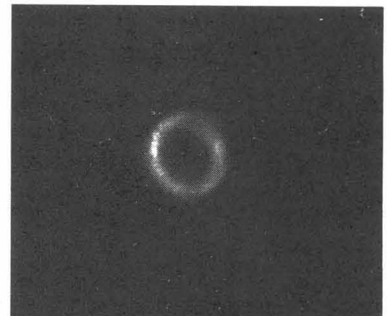

Fig. 9. Time-integrated pinhole photograph of the beam from the new injector. The slight ellipticity is due to a small parallax between the beam and camera axis.